International Journal of Robotics and Automation, Vol. 12, No. 4, 1997

A FRAMEWORK FOR OPTIMAL TRAJECTORY PLANNING FOR AUTOMATED SPRAY COATING

J.K. Antonio,* R. Ramabhadran,** and T.-L. Ling**

Abstract

Automated spray-coating operations are widely used in many consumer product industries. Robotic manipulators are employed in such spray-coating operations to traverse around the objects to be coated. Given the high degree of repeatability of such systems, proper selection of paths and other process parameters can result in significant cost savings, with improved performance. This paper provides a framework for optimal path/parameter selection in spray-coating applications. A parametric model for spray deposition is introduced, and an optimization framework is formulated for the selection of various parameters such as the spatial path, the velocity profile, the type of traversal, and the fan angle of the spray pattern. Examples of choosing such parameters through the optimization framework are illustrated for the coating of flat and curved surfaces. Proper choices of each parameter for different surfaces are discussed with the trade-offs involved. The methodology provided in this paper is ideal for use in off-line simulation tools used for process optimization studies.

Key Words

Path selection, optimization, spray coating

1. Introduction

High-quality paint finish is an important factor in the sales of many manufactured products. The perceived quality of products such as automobiles, appliances, and furniture can be strongly influenced by the quality of their painted surfaces. Spray applicators are commonly used in industry to apply paint to the surfaces of manufactured products. The task of consistently achieving high-quality finishes from spray applicator systems is complicated by the sensitivity of the coating process relative to environmental conditions (e.g., ambient temperature, barometric pressure, and relative humidity) and parameters associated with the spray system itself (e.g., position and orientation of the applicator, paint flow rate, and paint viscosity). (Refer to [1] for an extensive discussion of the parameters associated with the spray-coating process.

In very general terms, the process of spray coating involves, first, the atomization and then spraying of a coating material (e.g., paint) towards a surface to be coated. Paints typically contain some type of solvent. As the solvent evaporates, liquid paint becomes more viscous; it eventually becomes solid when all solvent has evaporated. As atomized droplets of paint are transported through the air from the applicator to the surface, a relatively large fraction of solvent evaporates from the droplets, because the ratio of surface area to volume is relatively high for small droplets. Therefore, by the time droplets strike the surface their viscosities are substantially larger than they were immediately after atomization. This increase in viscosity helps to prevent the paint from running and/or sagging on the surface [2].

The complex interactions among the many parameters in a spray-painting system are not well understood. Even heavily automated spray-painting processes, such as those found in the automotive industry, are typically designed or tuned based on "rules of thumb" [3]. It is common practice for such painting facilities to initially set some of the system parameters (such as shaping air pressure, paint flow rate, solvent concentration, and applied electrostatic voltage) by spraying several dozen "test panels" under various values for these parameters. A jury of paint experts then convenes to examine the painted test panels and vote to establish a rank ordering of the panels based on a weighted collection of quality attributes. The parameter settings associated with the panel with the highest overall ranking are then used as set points on the production line for that day (or shift). Because a human's ability to make consistent judgements regarding paint quality are strongly influenced by his or her mood, levels of fatigue, and other factors, some facilities incorporate the use of optical/image sensing devices and signal processing techniques to automate the process of judging test panels [4, 5].

The hue of a surface that is coated with a coloured paint depends, to a degree, on the film thickness of the paint. In particular, the film should be sufficiently thick that it "hides" the influence of the colour associated with the underlying primer coating (or the colour of the surface itself if no primer coating is present). Thus, one way to produce a uniform hue across a surface is to accumulate a sufficient amount of film thickness at each surface point, that is, enough thickness at each surface point to hide the primer. However, this approach can result in wasted paint if film thickness is not kept uniform across the surface. Also, those portions of the film that are too thick have the undesirable tendency to crack in use [6]. Thus, minimizing the variation in film thickness not only produces a more uniform hue across the entire surface, but can also improve the "structural integrity" of the finish.

In this paper, the question of how to optimally tra-

* Department of Computer Science, Texas Tech University, MS 3104, Lubbock, TX, USA 79409-3104; e-mail: antonio@ttu.edu

** School of Electrical and Computer Engineering, Purdue University, 1285 Electrical Engineering Building, West Lafayette, IN 47907-1285 USA

(paper no. 95-064)

verse a spray applicator around a surface to be coated is formulated as a type of optimization problem known as a constrained variational problem. An optimal trajectory is defined here as one that results in minimal variation in film thickness on the surface. Although factors other than uniformity of film thickness contribute to the overall quality of the finish, minimizing variation in film thickness is known to be a desirable property for many applications (see, e.g., [4, 6]). (Refer to [7] for a discussion of other possible metrics, such as distinction of image (DOI) and aesthetic defects.)

The trajectory for an applicator is defined by a six-dimensional vector function that specifies the position and orientation of the applicator at each instant of time. The surface to be coated is assumed to be represented by a set of points. For each surface point and for each feasible position and orientation of the applicator, a value for the instantaneous rate of film accumulation is assumed to be known. Empirical data and/or estimates for these values can be readily incorporated in the formulation (i.e., an analytic functional representation need not be known).

From a practical viewpoint, it is desirable for a trajectory optimization technique to be able to utilize empirical data for film accumulation rates because such data can be obtained through off-line experimentation. For example, based on a representative collection of positions and orientations for the spray applicator relative to a given surface, corresponding film thickness measurements can be made to estimate the rate of film accumulation at each surface point. That is, film thickness measurements could be taken after spraying paint for a small (and known) amount of time from each feasible position and orientation. Both dry- and wet-film gauges can be used to measure film thickness. (For a detailed description of such devices, refer to [6, 7].)

The remainder of this paper is organized as follows. In Section 2, a model for the spray-coating process is described and some associated notations are introduced. The mathematical formulation of the optimal trajectory planning problem is developed in Section 3. In Section 4 solution techniques for the formulated optimization problem are developed. Section 5 includes numerical studies that demonstrate the effectiveness of standard optimization techniques. The numerical studies focus on an important practical situation in which the spatial path is assumed to be specified and the optimization approach is applied to determine how to best traverse the path as a function of time. (Solution techniques for the more general problem of optimal spatial path selection are outlined in Section 4.) A summary and some concluding remarks are included in the final section.

2. Modelling and Notation for Spray Coating

2.1 Models for the Surface and Applicator Trajectory

The surface to be coated is defined by a set of points $\mathcal{S} \subset \mathcal{R}^3$, measured with respect to a fixed reference frame. Associated with each surface point $\mathbf{s} \in \mathcal{S}$ is a known unit normal vector $\mathbf{n}(\mathbf{s})$.

The position and "pointing orientation" (i.e., not angular orientation) of the applicator with respect to the same reference frame as the surface are defined, respectively, by two vectors: a three-dimensional position vector $\mathbf{p}(t)$ and a three-dimensional orientation vector $\mathbf{o}(t)$. These two vectors are defined at time t as:

$$\mathbf{p}(t) = [p_x(t) \;\; p_y(t) \;\; p_z(t)]',$$

$$\mathbf{o}(t) = [o_x(t) \;\; o_y(t) \;\; o_z(t)]'$$

The values $p_x(t)$, $p_y(t)$, and $p_z(t)$ represent the applicator's position at time t with respect to the fixed Cartesian reference frame XYZ. The values $o_x(t)$, $o_y(t)$, and $o_z(t)$ describe the applicator's orientation from its position with respect to the same fixed reference frame used by $\mathbf{p}(t)$. For convenience, a single vector $\mathbf{a}(t)$ is used to denote both the position and orientation of the applicator:

$$\mathbf{a}(t) = \begin{bmatrix} \mathbf{p}(t) \\ \mathbf{o}(t) \end{bmatrix}$$

2.2 The Rate of Film Accumulation

A general framework is proposed for modelling the rate at which film accumulates at each surface point. For the spray-coating problem, two general classifications can be made for models describing the rate of film accumulation. The first type of film accumulation rate function considered, called an infinite range model, has the feature that its value actually goes to zero only as the distance between the applicator and the point on the surface tends to infinity. Examples of this type are the bivariate Cauchy distribution considered in [8], and the bivariate Gaussian distribution considered in [9]. The advantages of using these functions are: (1) the surface integrals can be readily evaluated (thus saving some computation time); and (2) the induced cost functions are quite smooth, which generally enhances the convergence properties of most nonlinear programming algorithms that may be used to solve the resulting optimization problem.

The second type of film accumulation rate function used, called a finite range model, is a more accurate indicator of actual film accumulation rates, as the film accumulation rate function is zero for surface points that are outside a specific region surrounding the applicator's position. Such models can be specified based on empirical studies; an example is the model considered in [10]. In most finite-range models, the integration of the film accumulation rate function must be done numerically, and the associated cost functions are not as smooth as those generated by the infinite-range models. Thus, optimization studies involving these types of models tend to involve a higher computational burden.

The model developed in this subsection is of the finite-range type. It accounts for the relative orientation between the applicator and the surface, the distance between the applicator and the surface, the local curvature of the surface, the "fan angle" parameter of the applicator, and the flow rate of the paint entering the applicator. A schematic

overview of this model is shown in fig. 1.

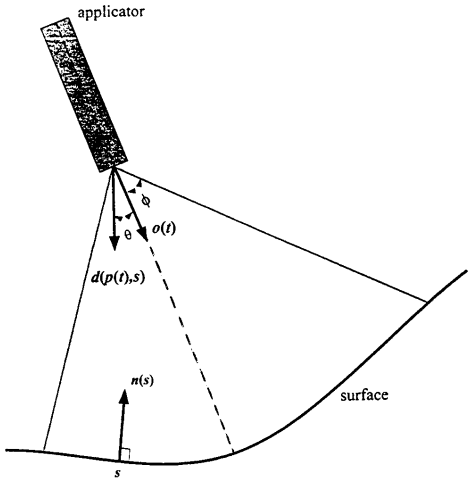

Figure 1. Diagram showing the parameters of the film accumulation model.

One important physical property to consider when modelling paint distributions is that the total amount of paint incident on the object (i.e., the total volume of paint released from the applicator) is independent of the geometry of the surface and the distance between the object and the applicator [1, 11]. The model developed here satisfies this property. The proposed expression for the rate of film accumulation at each surface point $\mathbf{s} \in \mathcal{S}$ is derived based on the following basic assumptions.

A1. Paint particles are emitted from the applicator radially within a circular cone with fan angle $\phi < 90°$ (refer to fig. 1 for a graphical definition of the parameter ϕ).

A2. Consider the set of points that are a distance $r > 0$ from the applicator and reside along the boundary of a circular cone with angle $\theta < \phi$. The density of paint particles at these points is given by:

$$\frac{c(\theta,\phi)}{r^2}$$

where $c(\theta,\phi)$ is a function that satisfies:

$$c(\theta,\phi)\begin{cases} > 0, & \theta < \phi \\ = 0, & \theta \geq \phi \end{cases}$$

A3. The rate of film accumulation at an arbitrary surface point $\mathbf{s} \in \mathcal{S}$, with a Cartesian coordinate representation $\mathbf{s} = (x, y, z)$, is proportional to the inner product between the unit normal vector at the surface point, denoted $\mathbf{n}(\mathbf{s})$, and the directional vector $\mathbf{d}(\mathbf{p}(t), \mathbf{s})$, which is defined as the unit vector from the applicator's source to the surface point (refer to fig. 1):

$$\mathbf{d}(\mathbf{p}(t),\mathbf{s}) = \frac{(x - p_x(t))\mathbf{i} + (y - p_y(t))\mathbf{j} + (z - p_z(t))\mathbf{k}}{\sqrt{(x - p_x(t))^2 + (y - p_y(t))^2 + (z - p_z(t))^2}} \quad (1)$$

where $\mathbf{i}$, $\mathbf{j}$, and $\mathbf{k}$ are unit vectors along the X, Y, and Z coordinates, respectively.

Based on the above assumptions, the rate of film accumulation for each surface point $\mathbf{s}$, denoted by $\dot{f}_{\mathcal{S}}(\mathbf{a}(t), \phi, \mathbf{s})$, is defined by:

$$\dot{f}_{\mathcal{S}}(\mathbf{a}(t),\phi,\mathbf{s}) = \left(\frac{c(\theta,\phi)}{(x - p_x(t))^2 + (y - p_y(t))^2 + (z - p_z(t))^2}\right) \mathbf{d}(\mathbf{p}(t),\mathbf{s}) \cdot \mathbf{n}(\mathbf{s}) \quad (2)$$

The dependence on θ is not explicitly noted as an argument of $\dot{f}_{\mathcal{S}}(\mathbf{a}(t), \phi, \mathbf{s})$ because the value of θ associated with each surface point $\mathbf{s}$ is defined by the position and orientation of the applicator, that is:

$$\theta = \cos^{-1}(\mathbf{d}(\mathbf{p}(t),\mathbf{s}) \cdot \mathbf{o}(t))$$

Similar models that are based on an inner product form have been proposed in the past. For example, in [1] the surface is discretized into small nonoverlapping triangles and the normal vector for each triangle is used similar to the way $\mathbf{n}(\mathbf{s})$ is used here. The choice for the function $c(\theta,\phi)$ depends on the general characteristics of the spray applicator and the values of parameter settings such as shaping air pressure and paint flow rate. Typically, the function has a maximum value when $\theta = 0$ and approaches zero smoothly as $\theta \to \phi$ [10]. An example of a typical function is given by:

$$c(\theta,\phi) = \begin{cases} \alpha \frac{\cos(\theta) - \cos(\phi)}{(1 - \cos(\phi))^2}, & \text{for } \theta \leq \phi \\ 0, & \text{otherwise} \end{cases}$$

For the above function, parameters such as the paint flow rate and shaping air pressure can be accommodated by adjusting the values of α and ϕ, respectively. Note that α corresponds to the maximum amplitude of the function. Other functions such as Gaussian and beta distributions have also been used (see, e.g., [1]).

3. The Optimal Trajectory Planning Problem

3.1 The Objective of the Optimal Trajectory Planning Problem

The objective of the optimal trajectory planning problem is to determine a trajectory that results in minimal variation in accumulated film thickness on the surface. The specific objective used here is the mean squared error between actual film thickness and average film thickness across the surface.

For a trajectory $\mathbf{a}(t)$ defined over a time interval $[0, T]$, the film thickness accumulated during the time interval $[0, T]$ at each point $\mathbf{s}$ on the surface $\mathcal{S}$ is given by:

$$f_{\mathcal{S}}(\mathbf{a}(t),\phi,\mathbf{s}) = \int_0^T \dot{f}_{\mathcal{S}}(\mathbf{a}(t),\phi,\mathbf{s})\, dt \quad (3)$$

In the above equation, recall that ϕ denotes the fan angle of the spray cone. This parameter is assumed constant over a given traversal around the surface to be coated. Conceptually, this parameter could be considered to be a function of time and/or an optimization variable. This is not considered here because it is generally difficult or impractical to accurately control (i.e., vary) this parameter over time.

Owing to integration over time, the accumulated film thickness $f_S(\mathbf{a}(t), \phi, \mathbf{s})$ does not depend explicitly on t; however, it does depend on the vector function of time $\mathbf{a}(t)$. The total volume of paint deposited onto the surface is given by:

$$F_S(\mathbf{a}(t), \phi) = \int_S f_S(\mathbf{a}(t), \phi, \mathbf{s}) d\mathbf{s} \tag{4}$$

If the values for $\dot{f}_S(\mathbf{a}(t), \phi, \mathbf{s})$ are derived from a collection of experimentally measured data values or not expressed analytically, then the integration required in (3) and (4) can be approximated numerically by using standard numerical integration techniques. Note that the model assumed here does not explicitly model the fact that some paint particles will be "lost in the air."

The average film thickness over the surface, denoted as $f_S^{\text{avg}}(\mathbf{a}(t), \phi)$, is defined as the total volume of paint deposited onto the surface divided by the area of the surface:

$$f_S^{\text{avg}}(\mathbf{a}(t), \phi) = \left(\frac{1}{A_S}\right) F_S(\mathbf{a}(t), \phi) \tag{5}$$

where the area of the surface is given by:

$$A_S = \int_S d\mathbf{s} \tag{6}$$

The variation in film thickness for the surface, denoted by $V_S(\mathbf{a}(t), \phi)$, is defined as the mean squared error between film thickness at each point and average film thickness:

$$V_S(\mathbf{a}(t), \phi) = \frac{1}{A_S} \int_S \left(f_S(\mathbf{a}(t), \phi, \mathbf{s}) - f_S^{\text{avg}}(\mathbf{a}(t), \phi)\right)^2 d\mathbf{s} \tag{7}$$

The optimal trajectory problem involves finding a trajectory $\mathbf{a}(t)$ that minimizes the variation in film thickness defined by (7). The average thickness can be adjusted by controlling the length of the time interval over which the trajectory is defined (i.e., T).

3.2 Practical Constraints for the Optimal Trajectory Planning Problem

In practice, there are constraints on the set of trajectories that are feasible associated with realistic robotic manipulators. In particular, there are constraints on the set of positions and orientations that are "reachable" by a given robotic system. There are also limits associated with the velocities and accelerations that can be developed to move the applicator along a reachable path. For example, large accelerations in one of the components of $\mathbf{a}(t)$ can imply large input torque requirements for the joint actuators, which can be difficult to realize in practice. (For more details on tracking trajectories in the presence of such constraints, refer to [12, 13].)

In addition to the constraints imposed by the robotic manipulator itself, in practice it may be desirable actually to further constrain the collection of feasible trajectories. For instance, in some applications it may be practical to consider only those trajectories where the applicator's positions are within a range of distance (e.g., between 8 and 12 inches) from the surface or consider only orientations where the centreline of the applicator's spray pattern is normal to the surface. Adding such intuitive constraints decreases the size of the search space, may improve the quality of the obtained solution, and increases the possibility of attaining a globally optimal solution.

An extreme form of the optimal trajectory planning problem is to constrain the movement of the applicator to be along a specified spatially continuous path. Thus, the objective for this case is to determine the optimal *time profile* for traversing the specified *spatial path*. In this case, it is possible to parameterize the continuous set of positions and orientations with a scalar variable. Thus, instead of having up to six optimization variables at each time instant (one for each degree of freedom for position and orientation), we need to determine only the time function of the scalar parameterizing variable.

In the next section, the optimal trajectory planning problem along a specified spatial path is formulated. Then, in Section 3.4, the optimal trajectory planning problem is formulated for the case where the constraints on the trajectory are more general (i.e., the spatial components of the trajectory are not completely specified). Finally, in Section 3.5 we note that the formulated optimal trajectory planning problems belong to a well-known class of optimization problems, and provide some general background for this class of optimization problems.

3.3 The Optimal Trajectory Planning Problem along a Specified Spatial Path

In large-scale production lines, robots are often used to position and move spray applicators around surfaces to be painted. In such an environment, it is common practice for an operator to literally "teach" the robot a spatial path by grasping the end-effector and manually moving the end-effector around the part to be painted while the robot's control computer records position and orientation information [7]. Having stored the path information, the robot can then repeatedly traverse the "learned" spatial path using a time profile specified by the operator.

In general, the accumulated film thickness of a target area is proportional to the amount of time spent spraying the area. Therefore, moving the applicator more slowly over certain regions may be called for if the spatial path is such that there is very little accumulation contributed to the area by other positions on the path. There can be trade-offs between achieving uniform coatings and minimizing wasted paint, especially when traversing near the edges of a part [8, 9, 14].

The positions and orientations along a specified spatial path can be characterized by a continuous vector function $\mathbf{g}(\rho)$, where ρ is a real scalar parameter, $0 \leq \rho \leq 1$. The first three elements of $\mathbf{g}(\rho)$ define the position of the applicator and the second three elements define its orientation. To model the motion of the applicator along a parameterized path during the time interval $[0, T]$, the scalar quantity ρ is replaced by a function of time $\lambda(t)$, where $\lambda : [0, T] \rightarrow [0, 1]$. Therefore, the position and orientation of the applicator at each instant of time are specified by $\mathbf{a}(t) = \mathbf{g}(\lambda(t))$. The function $\lambda(t)$ is referred to as the time profile of the applicator.

For practical reasons, it is generally necessary to constrain $\lambda(t)$ to be a continuous function in order to prevent discontinuous movements of the applicator (recall that $\mathbf{g}(\rho)$ is also assumed to be continuous in ρ). It may further be necessary to limit the values of the first and second derivatives of $\lambda(t)$ in order to constrain the speed and acceleration of the applicator. For notational convenience, let $\Lambda(t)$ be the set of all $\lambda(t)$'s that satisfy all such constraints.

Thus, the optimal trajectory planning problem along a given spatially parameterized path $\mathbf{g}(\cdot)$ is an optimization problem of the form:

$$\min_{\lambda(t) \in \Lambda(t)} \{V_{\mathcal{S}}(\mathbf{g}(\lambda(t)), \phi)\} \tag{8}$$

3.4 The Optimal Trajectory Planning Problem with General Constraints

In the general case, the feasible constraint set can include trajectories that do not share the same spatial path. Let $\mathbf{A}(t)$ denote a general set of feasible applicator trajectories. Thus, $\mathbf{A}(t)$ is a set of six-dimensional vector functions of time. In practice, the union of all spatial points associated with all vector functions in $\mathbf{A}(t)$ is constrained by the region that is reachable by the robotic manipulator. Also, the translational and/or rotational velocities of the trajectories in $\mathbf{A}(t)$ may be constrained.

Therefore, the optimal trajectory planning problem with general constraints is an optimization problem of the form:

$$\min_{\mathbf{a}(t) \in \mathbf{A}(t)} \{V_{\mathcal{S}}(\mathbf{a}(t), \phi)\} \tag{9}$$

In contrast to the optimal trajectory planning problem along a specified spatial path (where the search space is over a set of scalar functions of time), the optimization problem defined in (9) generically requires a search over a set of six-dimensional vector functions of time.

3.5 Classification of Optimal Trajectory Planning Problems

The optimal trajectory planning problem along a specified spatial path and the optimal trajectory planning problem with general constraints both belong to a general class of optimization problems known as constrained variational problems [15]. Constrained variational problems are analogous to, but more general than, problems that involve optimizing an ordinary function of several variables with constraints. Unlike the problem of optimizing an ordinary function $f(\mathbf{x})$ over a constraint set $\mathbf{X}$ (where the objective is to determine a vector $\mathbf{x}^* \in \mathbf{X}$ such that $f(\mathbf{x}^*) \leq f(\mathbf{x})$, for all $\mathbf{x} \in \mathbf{X}$), variational problems involve determining functions that minimize a given function of functions. Thus, in variational problems vector functions are sought that minimize a given functional. For the optimal trajectory planning problem of (8), a scalar function $\lambda(t) \in \Lambda(t)$ is sought to minimize the functional $V_{\mathcal{S}}(\mathbf{g}(\lambda(t)), \phi)$. For the optimal trajectory planning problem of (9), a vector function $\mathbf{a}(t) \in \mathbf{A}(t)$ is sought to minimize the functional $V_{\mathcal{S}}(\mathbf{a}(t), \phi)$.

Analogous to how an extremum for an ordinary function can be determined by setting the gradient of the function to zero, the extremum of a functional can be determined by setting the "variation" of the functional to zero. Although the precise definition for the variation of a functional will not be given here (because it is not required for the solution techniques used in this paper), note that an extremum function of a functional is the solution to a set of nonlinear differential equations that results from setting the variation of the functional to zero. Determining solutions for nonlinear differential equations is generally more complicated than determining solutions for the nonlinear algebraic equations associated with setting the gradient of an ordinary function to zero.

Because the differential equations associated with setting the variation of a functional to zero are rarely easy to integrate, other, more practical approaches have been devised in the literature. One way to determine solutions to variational problems is to employ a so-called direct method. The basic idea underlying direct methods is to consider a variational problem as a limit problem for some problem of extrema of a function of a finite number of variables [15]. The techniques described in the next section for solving the optimal trajectory problem are examples of direct methods.

4. Solution Techniques for Optimal Trajectory Planning Problems

4.1 Solving the Optimal Trajectory Planning Problem along a Specified Spatial Path

The proposed technique for solving the optimization problem of (8) is based on approximating $\lambda(t)$ as a piecewise constant function. Divide the interval $[0, T]$ into N subintervals, each of width $\Delta = T/N$. Let $b_k(t)$ denote a "boxcar" function, which is defined for each $k \in [1, 2, \ldots, N]$ as follows:

$$b_k(t) = \begin{cases} 1 & \text{if } t \in [(k-1)\Delta, k\Delta] \\ 0 & \text{otherwise} \end{cases} \tag{10}$$

Thus, a piecewise constant approximation for $\lambda(t)$ is given by:

$$\tilde{\lambda}(t) = \sum_{k=1}^{N} \lambda_k b_k(t) \approx \lambda(t) \tag{11}$$

where $\lambda_k \in [0,1]$ represents the constant value of $\tilde{\lambda}(t)$ over the subinterval $[(k-1)\Delta, k\Delta]$.

If we replace $\mathbf{a}(t)$ with $\mathbf{g}(\tilde{\lambda}(t))$ in the right side of (3), the approximation for film thickness becomes:

$$\tilde{f}_S(\lambda,\phi,\mathbf{s}) = \Delta \sum_{k=1}^{N} \dot{f}_S(\mathbf{g}(\lambda_k),\phi,\mathbf{s}) \approx f_S(\mathbf{g}(\lambda(t)),\phi,\mathbf{s}) \tag{12}$$

where $\lambda = [\lambda_1 \lambda_2 \cdots \lambda_N]'$. Likewise, the corresponding approximation for the variation in film thickness is given by:

$$\tilde{V}_S(\lambda,\phi) = \frac{1}{A_S}\int_S \left(\tilde{f}_S(\lambda,\phi,\mathbf{s}) - \tilde{f}_S^{\text{avg}}(\lambda,\phi)\right)^2 ds \approx V_S(\mathbf{g}(\lambda(t)),\phi) \tag{13}$$

where:

$$\tilde{f}_S^{\text{avg}}(\lambda,\phi) = \frac{1}{A_S}\int_S \tilde{f}_S(\lambda,\phi,\mathbf{s})\, ds \approx f_S^{\text{avg}}(\mathbf{g}(\lambda(t)),\phi) \tag{14}$$

The function $\tilde{V}_S(\lambda,\phi)$ represents an approximation to the objective functional associated with the original variational problem of (8). Of course, the constraints defining the allowable set of functions from the original variational problem, that is, $\Lambda(t)$, must also be transformed into a suitable constraint set for the vector λ. Clearly, the range of values for λ_k is bounded by $0 \le \lambda_k \le 1$, for all $k \in [1,2,\ldots,N]$. Also, in order to limit the speed to the feasible applicator trajectories, constraints may be placed on $|\lambda_k - \lambda_{k+1}|$, for each $k \in [1,2,\ldots,N-1]$. Denote the set of vectors that satisfy all such constraints on the vector λ by $\mathbf{\Lambda}$.

Thus, the nonlinear programming approximation to the optimal trajectory planning problem along a spatially parameterized path $\mathbf{g}(\cdot)$ has the form:

$$\min_{\lambda\in\mathbf{\Lambda}}\{\tilde{V}_S(\lambda,\phi)\} \tag{15}$$

Provided that the function $\tilde{V}_S(\lambda,\phi)$ is differentiable, standard nonlinear programming techniques (e.g., gradient descent algorithms) can be employed to provide solutions to the optimization problem stated in (15) [16]. If the gradient of the objective function, that is, $\nabla\tilde{V}_S(\lambda,\phi)$, cannot be expressed analytically, then it can be approximated numerically. Examples of this problem are solved in Section 5 by the quasi-Newton method with a finite-difference approximation for the gradients. A particular routine used in the numerical studies (in Section 5) is the BCONF routine from IMSL [17].

4.2 Solving the Optimal Trajectory Planning Problem with General Constraints

Analogous to the technique of Section 4.1, the technique proposed here for solving the optimization problem of (9) is based on approximating $\mathbf{a}(t)$ as a piecewise constant vector function. Again, the interval $[0,T]$ is divided into N subintervals each of width $\Delta = T/N$. The boxcar function $b_k(t)$ of (10) is used to define a piecewise constant approximation for $\mathbf{a}(t)$:

$$\hat{\mathbf{a}}(t) = \sum_{k=1}^{N} \mathbf{a}_k b_k(t) \approx \mathbf{a}(t) \tag{16}$$

where:

$$\mathbf{a}_k = [p_{x,k}\ \ p_{y,k}\ \ p_{z,k}\ \ o_{x,k}\ \ o_{y,k}\ \ o_{z,k}]' \tag{17}$$

Thus, the vector $\mathbf{a}_k$ represents the position and orientation of the applicator during the time interval $[(k-1)\Delta, k\Delta]$.

By replacing $\mathbf{a}(t)$ with $\hat{\mathbf{a}}(t)$ in the right side of (3), we can straightforwardly verify the following approximation for film thickness:

$$\hat{f}_S(\mathbf{a},\phi,\mathbf{s}) = \Delta \sum_{k=1}^{N} \dot{f}_S(\mathbf{a}_k,\phi,\mathbf{s}) \approx f_S(\mathbf{a}(t),\phi,\mathbf{s}) \tag{18}$$

where $\mathbf{a} = [\mathbf{a}_1'\mathbf{a}_2'\cdots\mathbf{a}_N']'$. Likewise, the corresponding approximation for the variation in film thickness is given by:

$$\hat{V}_S(\mathbf{a},\phi) = \frac{1}{A_S}\int_S \left(\hat{f}_S(\mathbf{a},\phi,\mathbf{s}) - \hat{f}_S^{\text{avg}}(\mathbf{a},\phi)\right)^2 ds \approx V_S(\mathbf{a}(t),\phi) \tag{19}$$

where:

$$\hat{f}_S^{\text{avg}}(\mathbf{a},\phi) = \frac{1}{A_S}\int_S \hat{f}_S(\mathbf{a},\phi,\mathbf{s})\, ds \approx f_S^{\text{avg}}(\mathbf{a}(t),\phi) \tag{20}$$

The function $\hat{V}_S(\mathbf{a},\phi)$ represents an approximation to the objective functional associated with the variational problem of (9). In contrast to the analogous approximation given in (13), which depends on the N-vector λ, the function $\hat{V}_S(\mathbf{a},\phi)$ generically depends on $6N$ variables because each of the N "components" of $\mathbf{a}$, that is, $\mathbf{a}_k$, is actually a six-dimensional vector.

The constraints on the feasible set of functions from the original variational problem, $\mathbf{A}(t)$, must be transformed into a suitable constraint set for the vector $\mathbf{a}$. Clearly, the range of values for each $\mathbf{a}_k$ is bounded by the set of reachable spatial points of the robotic manipulator. Also, constraints may be placed on translational and rotational speeds by bounding $[(p_{x,k}-p_{x,k+1})^2 + (p_{y,k}-p_{y,k+1})^2 + (p_{z,k}-p_{z,k+1})^2]^{\frac{1}{2}}$ and $[(o_{x,k}-o_{x,k+1})^2 + (o_{y,k}-o_{y,k+1})^2 + (o_{z,k}-o_{z,k+1})^2]^{\frac{1}{2}}$, respectively. Denote the set of vectors that satisfy all such constraints on $\mathbf{a}$ by $\mathbf{A}$.

Thus, the nonlinear programming approximation to the optimal trajectory planning problem with general constraints has the form:

$$\min_{\mathbf{a}\in\mathbf{A}}\{\hat{V}_S(\mathbf{a},\phi)\} \tag{21}$$

Analogous to the discussion of practical solution techniques for the optimization problem of (15), if the function $\hat{V}_S(\mathbf{a})$ is sufficiently smooth (i.e., differentiable), then

standard nonlinear programming techniques can also be employed to provide solutions to the optimization problem of (21).

5. Numerical Results

5.1 Overview

To demonstrate the utility of the optimization technique proposed in Section 4.1 (for traversing a specified spatial path), three example surfaces are considered: a flat panel, a convex panel, and a concave panel. The objective of the numerical studies is to evaluate, for a given spatial path $\mathbf{g}(\cdot)$, the optimal vector $\lambda = [\lambda_1 \lambda_2 \cdots \lambda_N]'$ that achieves the minimum variation in film thickness $\widetilde{V}_S(\lambda, \phi)$. For the flat panel, one spatial path is considered (see fig. 2). For each curved surface, two distinct types of paths are considered: a type 1 path, in which the applicator traverses "along the curvature" of the surface; and a type 2 path, in which the applicator traverses "across the curvature" of the surface. The type 1 path for a convex surface is shown in fig. 3 and the type 2 path for a convex surface is shown in fig. 4.

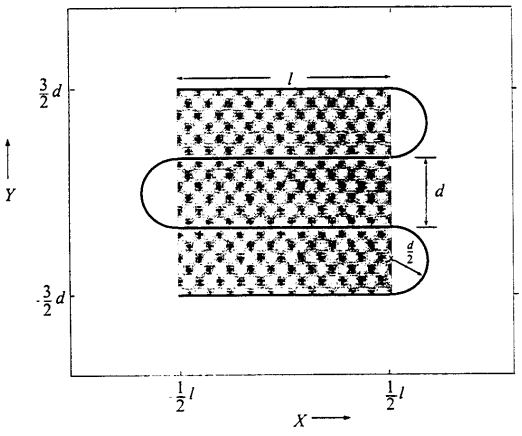

Figure 2. Spatial path of applicator over a flat panel (indicated by the shaded area).

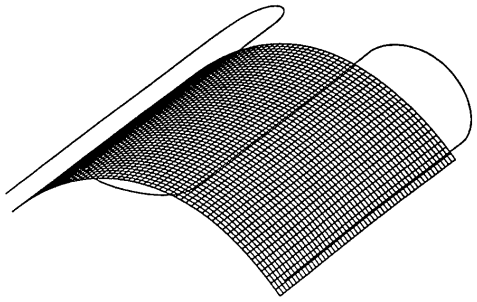

Figure 3. A type 1 path for a convex surface.

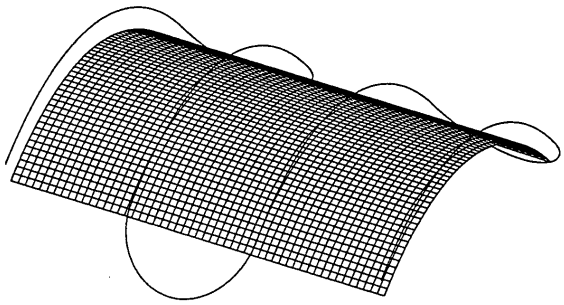

Figure 4. A type 2 path for a convex surface.

The fan angle ϕ of the spray cone is fixed for a given traversal. However, the effect of using different fan angle values for different trials is also evaluated as a part of the study. For each case considered, the evaluation is made complete by comparing the performance associated with the computed optimal traversal with the corresponding constant speed traversal using the same specified spatial path.

5.2 Traversal over a Flat Panel

The first surface considered is a square flat panel that is located within the XY plane. It is assumed that the applicator can be positioned above the panel so that the centreline of the spray pattern is oriented normal to the panel's surface. For convenience, the units of length are not specified here. In practice, the units for the dimensions of the panel may be on the order of a few feet or metres and the units for the rate of film accumulation, that is, $\dot{f}_S(\mathrm{a}(t), \phi, \mathrm{s})$, could be on the order of a μm/sec.

Fig. 2 shows the XY coordinates of both the flat panel and a parameterized spatial path, $\mathbf{g}(\rho)$. The value of ℓ is the length of each straight segment associated with the four horizontal "sweeps" over the panel and d is the indexing distance between consecutive sweeps. The endpoints of the horizontal segments are connected by semicircular arcs of radius $\frac{d}{2}$. The total length of the path is given by $L = 4\ell + \frac{3\pi d}{2}$. An analytical parameterization of the path of the form

$$\mathbf{g}(\rho) = [g_x(\rho) \;\; g_y(\rho) \;\; h \;\; 0 \;\; 0 \;\; -1]', \rho \in [0, 1]$$

where h denotes the constant distance of the applicator from the surface, is given in [8].

Results of the numerical studies on the flat panel are shown in table 1. For these studies, the fan angle parameter was set at $\phi = 45.5°$, and the parameters associated with the spatial path were $\ell = 5\frac{1}{3}, d = 1\frac{7}{9}$, and $h = 1$. We can see that the optimal time profile outperforms the constant speed solution with respect to both variation in film thickness and required painting time (recall that the objective was to minimize only variation in film thickness). Note that the variation in film thickness achieved by using the optimization technique is over an order of magnitude better than that associated with the constant speed

traversal. The tabulated values of painting time represent the time required to achieve a unit average thickness (i.e., $\tilde{f}_S^{\text{avg}}(\lambda,\phi) = 1$). The fact that the optimal traversal requires less time indicates that the applicator spends less time in areas where the transfer efficiency of paint to the surface is low (i.e., places where the applicator is not directly above the surface).

Table 1
Simulation Results for Flat Panel

Performance Indices	Traversal Method	
	Optimal	Constant Speed
Variation in film thickness, $\tilde{V}_S(\lambda,\phi)$ ($\times 10^{-3}$)	0.271	8.41
Painting time, T	5.73	5.84

Note. The fan angle was fixed for each traversal at $\phi = 45.5°$.

5.3 Traversal over a Convex Surface

The second type of surface considered is a convex surface. The surface can be visualized by bending a flat panel around a line segment parallel to the Y axis to a specified radius of curvature, denoted by R. The applicator is assumed to move on a hypothetical surface that is parallel to and at a distance h from the actual convex surface, preserving the normal orientation as in the case of the flat panel. The path of the applicator can be visualized by projecting the path used for the flat panel "outward" onto the hypothetical convex surface. The mathematically parameterized path used for the flat panel can be transformed to yield a parameterization for the path for the convex surface. In particular, the path for the convex surface is given

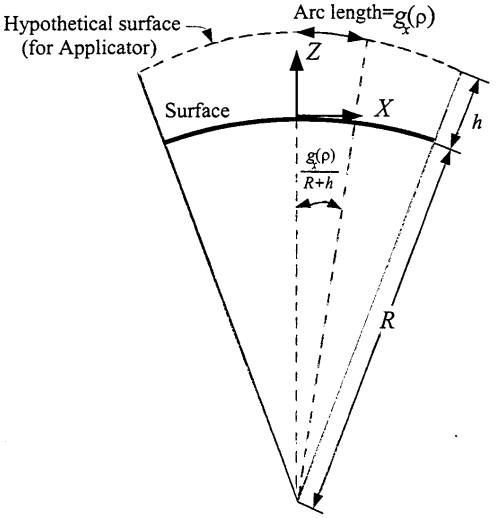

Figure 5. Transformation of the path over the flat panel to a path over a convex surface.

by (refer to fig. 5):

$$\mathbf{g}(\rho) = \left[(R+h)\sin\left(\frac{g_x(\rho)}{R+h}\right), g_y(\rho), (R+h)\cos\left(\frac{g_x(\rho)}{R+h}\right) - R, \sin\left(\frac{g_x(\rho)}{R+h}\right), 0, -\cos\left(\frac{g_x(\rho)}{R+h}\right)\right]'$$

Results of the numerical studies on the convex surface are shown in table 2. For these studies, the fan angle parameter was set at $\phi = 48.5°$, and the parameters used for the spatial path were $\ell = 5\frac{1}{3}, d = 1\frac{7}{9}, h = 1$, and $R = 5.3$. As in the case of the studies on the flat panel, the tabulated values of painting time represent the time required to achieve a unit average thickness (i.e., $\tilde{f}_S^{\text{avg}}(\lambda,\phi) = 1$). The variation in film thickness over the convex surface for an optimal traversal of a type 1 path is about five times smaller than that associated with a constant speed traversal of the same path. Traversing the surface with a type 2 path yields a variation in film thickness for an optimal traversal that is about 20 times smaller than that caused by a constant speed traversal of the same path. The painting time does not vary significantly, as indicated by the values in table 2. However, it is interesting to note that the type 2 path results in the smaller variation in film thickness and a shorter painting time.

5.4 Traversal over a Concave Surface

The third type of surface considered is a concave surface. The surface may be visualized as a flat panel bent "inward" to a specified radius of curvature, R, about a line segment parallel to the Y axis. The applicator is assumed to move on a hypothetical surface parallel to the concave surface, at a distance h, preserving the normal orientation as in the previous cases. The parameterized path used in the case of the flat panel is transformed to yield a similar parameterization for the spatial path over this surface (the derivation is similar to that for a concave surface). The parameterization for the path over the concave surface is given by:

$$\mathbf{g}(\rho) = \left[(R-h)\sin\left(\frac{g_x(\rho)}{R-h}\right), g_y(\rho), (R-h)\cos\left(\frac{g_x(\rho)}{R-h}\right) - h, \sin\left(\frac{g_x(\rho)}{R-h}\right), 0, -\cos\left(\frac{g_x(\rho)}{R-h}\right)\right]'$$

Results of the numerical studies for the concave surface are shown in table 3. The fan angle was kept fixed at a value of 43.5° throughout each traversal, and the parameters used for the spatial path were $\ell = 5\frac{1}{3}, d = 1\frac{7}{9}, h = 1$, and $R = 5.3$. The variation in film thickness for an optimal traversal of a type 1 path for the concave surface is about 13 times smaller than that resulting from a constant speed traversal of the same path. For the type 2 path, the optimal traversal yields a variation in film thickness that is about 10 times smaller than that caused by a constant speed traversal. In contrast to the convex case (see previous section), the type 1 path produces superior variation values for the concave surface.

Table 2
Simulation Results for Convex Surface

Performance Indices	Type 1 Path		Type 2 Path	
	Optimal	Constant Speed	Optimal	Constant Speed
Variation in film thickness, $\bar{V}_g(\lambda,\phi)$ ($\times 10^{-3}$)	1.87	9.54	0.31	7.26
Painting time, T	6.04	5.98	5.83	5.95

Note. The fan angle was fixed at a value of 48.5°.

Table 3
Simulation Results for Concave Surface

Performance Indices	Type 1 Path		Type 2 Path	
	Optimal	Constant Speed	Optimal	Constant Speed
Variation in film thickness, $\bar{V}_g(\lambda,\phi)$ ($\times 10^{-3}$)	0.69	9.58	1.09	9.97
Painting time, T	5.57	5.83	5.64	5.82

Note. The fan angle is kept fixed at a value of 43.5°.

5.5 Comparison of Path Lengths

In the previous subsections, we showed that choosing a type 2 path yields a better variation in film thickness for a convex surface and choosing a type 1 path yields a better variation in film thickness for the concave surface. Here we show that the path lengths for each case are different, and consequently the average velocities of the applicator over the surfaces turn out to be different. The path lengths for each type of traversal for the three surfaces considered are shown in table 4. For the flat panel, both traversal types have the same path length because the panel is square (i.e., symmetric). For the convex surface, the type 2 path is longer than the type 1 path. The type 2 path also has a higher average velocity for an optimal traversal (the average velocity is defined by dividing the length of the path by the total required painting time). Thus, the smaller variation in film thickness associated with the type 2 traversal over the convex surface is accompanied by an increased length of travel and a higher average velocity for the applicator. For the concave surface, the type 1 path was found to yield a better variation in film thickness. A comparison of path lengths indicates that the type 1 path is longer than the type 2 path for the concave surface. Further, the average velocity for the optimal traversal is higher for the type 1 path, for the concave surface. Thus, for both the concave and the convex surfaces, the longer path (type 1 for concave and type 2 for convex), with a higher average velocity yields lower variations in film thickness, at a "price" of requiring higher average velocities.

5.6 Effects of Changing the Fan Angle Parameter

In addition to the spatial path, another parameter that can be changed is the fan angle parameter ϕ. In the simulation studies discussed previously for the three types of surfaces, the fan angle parameter is kept constant for each traversal. To illustrate the effect of changing this parameter, numerical studies are conducted by fixing the fan angle parameters at various values. The results of these studies for the concave surface are illustrated in fig. 6. Plotted in the figure are the optimal variation in film thickness values (determined through numerical optimization studies) for various values of the fan angle parameter for a type 1 path. We can see that the variation in film thickness is the least for the fan angle of 42.5°. Intuitively, a low fan angle parameter value causes the surface to be improperly covered by the spray cone, which can cause a "striping" effect (and thus unavoidably high variation values). A high fan angle value tends to cause an overspray effect, which can also increase the variation in film thickness.

Table 4
Comparison of Path Lengths and Average Velocities for Both Traversals for the Three Surfaces Considered

Surface	Path Length		Average Velocity	
	Type 1 Path	Type 2 Path	Type 1 Path	Type 2 Path
Flat	29.71	29.71	5.19	5.19
Convex	30.51	34.69	5.05	5.95
Concave	28.93	25.45	5.19	4.51

Note. Average velocities are for the optimal traversals.

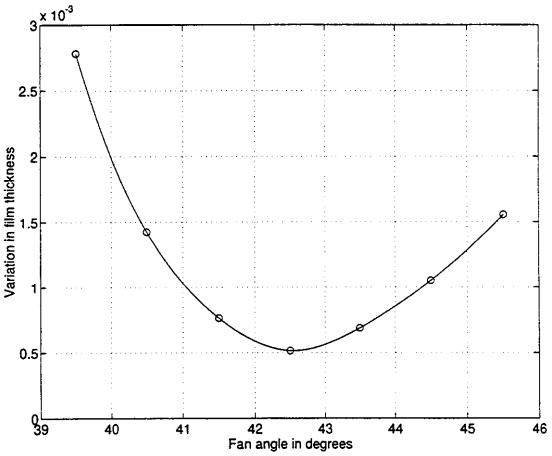

Figure 6. Effect of fan angle value on the optimal value of the variation in film thickness for a concave surface using a type 1 path.

6. Conclusion

We have developed a framework for solving optimal trajectory planning problems for spray coating. The proposed methodology is general in the sense that no real limitations are placed on the spray-coating system nor the surface to be coated. The methodology can utilize empirically based information for the rate of film accumulation at each surface point, as a function of the position and orientation of the applicator. We demonstrated through numeri-

cal studies that standard commercially available nonlinear programming algorithms can be applied to provide solutions for the formulated optimization problem.

The metric optimized in this paper is variation in film thickness, as defined by (7). This choice was made partly because of mathematical convenience (i.e., its smoothness lends itself to the employed nonlinear programming techniques). However, other metrics such as maximum deviation from the average may also be of practical interest. Preliminary investigation has been conducted by computing the value for the maximum deviation from the average for each solution given in tables 1, 2, and 3. As might be expected, it was discovered that the value of the maximum deviation from the average was strongly correlated with the tabulated values of variation in film thickness, for the cases considered. Future work may involve providing a more formal mathematical proof of this apparent correlation.

Future work may also include utilizing the techniques developed here as the basis for an interactive and graphically based tool for trajectory planning. A similar tool for this purpose was developed in [14]; however, the assumed spray pattern is more restrictive than the model developed here. Thus, our more general formulation provides a more realistic basis for simulation and optimization.

The optimal trajectory planning problem with general constraints (i.e., where both the spatial and temporal components of the trajectory are sought) may prove to be computationally intractable because of the complexity of the associated constraint set. In practice, an approach that allows the operator to specify the spatial path and uses the proposed optimization technique to determine how to traverse the path as a function of time shows great promise. A graphically based tool would enable the operator to evaluate the merit of several trajectories through off-line simulation.

Acknowledgements

This work was supported by the National Science Foundation under grant 8803017-ECD to the Engineering Research Center for Intelligent Manufacturing Systems. The authors thank Simon P. Yeung for his assistance in developing the software for the simulation studies. Preliminary versions of portions of the material in this paper were presented at the IEEE International Conference on Robotics and Automation, May 1994.

References

[1] W. Persoons & H.V. Brussel, CAD-based robotic coating of highly curved surfaces, *Proc. 24th Int. Symp. on Industrial Robotics (ISIR)*, November 1993, 611–618.

[2] D.A. Ansdell, Automotive paints, in R. Lambourne (ed.), *Paint and surface coatings: Theory and practice* (New York: Wiley, 1987), 431–489.

[3] H.E. Snyder, D.W. Senser, A.H. Lefebvre, & R.S. Coutinho, Drop size measurements in electrostatic paint sprays, *IEEE Trans. Industry Applications, 25*(4), July/August 1989, 720–727.

[4] J.K. Antonio, J.G. Wendelberger, G.P. Matthews, W.G. Trabold, & M.H. Costin, Optiscan: the use of reflectometry for detecting quality attributes of basecoat paint, General Motors Research Laboratories, Warren, MI, Research Report No. ET-426/MA-357, December 1986.

[5] H.H. Kuo & J.G. Wendelberger, GM-ORACLE II: Computer simulation of paint spray patterns, General Motors Research Laboratories, Warren, MI, Research Report No. PO-769, April 1986.

[6] G.L. Schneberger, *Understanding paint and painting processes*, 4th ed. (Carol Stream, IL: Hitchcock Publishing, 1989).

[7] M. Modesto & D. Sergio, Inspection and control systems for car body painting, *Proc. 23rd Int. Symp. on Industrial Robotics (ISIR)*, October 1992, 697–707.

[8] J.K. Antonio, Optimal trajectory planning for spray coating, Purdue University, School of Electrical Engineering, Technical Report No. TR-EE-93-29, September 1993, (Portions also published in *Proc. 1994 IEEE Int. Conf. on Robotics and Automation*, May 1994, 2570–2577).

[9] H. Hyötyiemi, Minor moves—global results: Robot trajectory planning, *Proc. 1990 IEEE Conf. on Decision and Control*, December 1990, 16–22.

[10] A. Klein, CAD-based off-line programming of painting robots, *Robotica (1987)*, vol. 5, 267–271.

[11] A.H. Lefebvre, *Atomization and sprays* (New York: Hemisphere Publishing, 1989).

[12] C.S.G. Lee & B.H. Lee, Resolved motion adaptive control for mechanical manipulators, *ASME J. Dynamic Systems, Measurements and Control, 106*, June 1984, 134–142.

[13] J.Y.S. Luh, M.W. Walker, & R.P.C. Paul, Resolved-acceleration control of mechanical manipulators, *IEEE Trans. Automatic Control, AC-25*, June 1980, 468–474.

[14] S.-H. Suh, I.-K. Woo, & S.-K. Noh, Development of an automatic trajectory planning system (ATPS) for spray painting robots, *Proc. 1991 IEEE Int. Conf. on Robotics and Automation*, April 1991, 1948–1955.

[15] L.E. Elsgolc, *Calculus of variations* (Reading, MA: Addison-Wesley, 1962).

[16] M.S. Bazaraa, H.D. Sherali, & C.M. Shetty, *Nonlinear programming: Theory and algorithms*, 2nd ed. (New York: Wiley, 1993).

[17] *IMSL Math-Library, Version 1.1, Volume 3*, IMSL Corporation, Houston, TX, Jan. 1989, 847–852.

Biographies

John K. Antonio received the B.Sc., M.Sc., and Ph.D. degrees in electrical engineering from Texas A&M University, College Station, TX. He currently holds the position of Associate Professor of Computer Science within the College of Engineering at Texas Tech University. Before joining Texas Tech, he was with the School of Electrical and Computer Engineering at Purdue Uni-

versity. During the summers of 1991–94 he participated in a faculty research program at Rome Laboratory, Rome, NY. His current research interests include computational aspects of control and optimization, and high-performance architectures for embedded systems. He has co-authored over 50 publications in these and related areas. He is a member of the IEEE computer and control systems societies and is also a member of the Tau Beta Pi, Eta Kappa Nu, and Phi Kappa Phi honorary societies. Organizations that have supported his research include the Air Force Office of Scientific Research, National Science Foundation, Naval Research Laboratory, ORINCON, Inc., and Rome Laboratory.

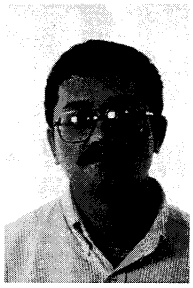

Ramanujam Ramabhadran was born in Madras, India. He obtained his B.E. in electrical and electronics engineering from Coimbatore Institute of Technology in 1990 and then worked as an installation engineer with Carborundum Universal Ltd. until July 1991. He obtained his M.Sc. degree in electrical engineering from Purdue University in 1993, with a thesis on automatic generation control for interconnected power systems. He received his Ph.D. in electrical engineering from Purdue in May 1997. Since January of 1996 he has been with the Process Engineering Group in Cummins Engine Co., Columbus, IN. His current research interests include modelling and control of finishing and nontraditional machining processes, distributed control for manufacturing, and open architecture control systems. He is a member of the Eta Kappa Nu honorary society.

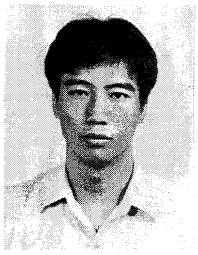

Ting-Li Ling was born in Taipei, Taiwan. He received his B.Sc. degree in electrical engineering from National Taiwan University, Taipei, Taiwan, in 1989. He obtained the M.Sc. and Ph.D. degrees in electrical engineering from Purdue University, West Lafayette, IN, in 1993 and 1997, respectively. He has since joined Pacific Bell in San Ramon, California, as a principal member of its technical staff. His current research interests include traffic management, scheduling and flow control in ATM networks, service requirements and deployment of ADSL, and service requirements development in support of network layer protocols over ATM. He is a member of the Eta Kappa Nu honorary society.